Developmental-stage-specific triacylglycerol biosynthesis, degradation and trafficking as lipid bodies in *Plasmodium falciparum*-infected erythrocytes

Nirianne Marie Q. Palacpac[1], Yasushi Hiramine[2], Fumika Mi-ichi[1,3,4], Motomi Torii[5], Kiyoshi Kita[4], Ryuji Hiramatsu[2], Toshihiro Horii[3] and Toshihide Mitamura[1,3,*]

[1]PRESTO, Japan Science and Technology Corporation, 4-1-8 Honcho Kawaguchi, Saitama 332-0012, Japan
[2]Sumitomo Chemical, 4-2-1 Takatsukasa, Takarazuka, Hyogo 665-0051, Japan
[3]Department of Molecular Protozoology, Research Institute for Microbial Diseases, Osaka University, 3-1 Yamadaoka, Suita, Osaka 565-0871, Japan
[4]Department of Biomedical Chemistry, Graduate School of Medicine, University of Tokyo, 7-3-1 Hongo, Bunkyou-ku, Tokyo 113-0033, Japan
[5]Department of Molecular Parasitology, Ehime University School of Medicine, Shigenobu-cho, Ehime 791-0295, Japan
*Author for correspondence (e-mail: mitamura@biken.osaka-u.ac.jp)

Accepted 13 November 2003
Journal of Cell Science 117, 1469-1480 Published by The Company of Biologists 2004
doi:10.1242/jcs.00988

Summary

Triacylglycerol (TAG) serves as a major energy storage molecule in eukaryotes. In *Plasmodium*, however, this established function of TAG appears unlikely, despite detecting previously considerable amount of TAG associated with intraerythrocytic parasites, because plasmodial cells have very little capacity to oxidize fatty acids. Thus, it is plausible that TAG and its biosynthesis in *Plasmodium* have other functions. As a first step in understanding the biological significance of TAG and its biosynthesis to the intraerythrocytic proliferation of *Plasmodium falciparum*, we performed detailed characterization of TAG metabolism and trafficking in parasitized erythrocyte. Metabolic labeling using radiolabeled-oleic and palmitic acids in association with serum albumin, which have been shown to be among the serum essential factors for intraerythrocytic proliferation of *P. falciparum*, revealed that accumulation of TAG was strikingly pronounced from trophozoite to schizont, whereas TAG degradation became active from schizont to segmented schizont; the consequent products, free fatty acids, were released into the medium during schizont rupture and/or merozoite release. These results were further supported by visualization of lipid bodies through immunofluorescence and electron microscopy. At the schizont stages, there is some evidence that the lipid bodies are partly localized in the parasitophorous vacuole. Interestingly, the discrete formation and/or trafficking of lipid bodies are inhibited by brefeldin A and trifluoperazine. Inhibition by trifluoperazine hints at least that a de novo TAG biosynthetic pathway via phosphatidic acid contributes to lipid body formation. Indeed, biochemical analysis reveals a higher activity of acyl-CoA:diacylglycerol acyltransferase, the principal enzyme in the *sn*-glycerol-3-phosphate pathway for TAG synthesis, at trophozoite and schizont stages. Together, these results establish that TAG metabolism and trafficking in *P. falciparum*-infected erythrocyte occurs in a stage-specific manner during the intraerythrocytic cycle and we propose that these unique and dynamic cellular events participate during schizont rupture and/or merozoite release.

Key words: Malaria, Nile Red, Neutral lipid, Acyl-CoA:diacylglycerol acyltransferase, Brefeldin A, Fatty acid

Introduction

Plasmodium falciparum is responsible for the most virulent form of malaria, a disease that exerts an enormous toll in terms of mortality and morbidity worldwide, particularly in Africa. In its life cycle, the parasite cell enters the intraerythrocytic stage, when the complexity of malaria pathogenesis appears. The dramatic increase in total lipid content of the infected erythrocyte is a significant feature associated with the intraerythrocytic *Plasmodium* parasites (Holz, 1977; Vial and Ancelin, 1998; Vial et al., 1982a; Vial et al., 1982b). Thus, the unique features in lipid metabolism and trafficking of *P. falciparum* have been attracting prompt attentions in lipid biology (Vial and Ancelin, 1998; Mitamura and Palacpac, 2003).

Triacylglycerol (TAG), which is usually found as concentrated cytoplasmic lipid droplets or oil bodies (Murphy and Vance, 1999), serves as highly reduced stores of oxidizable energy in most cells and is deemed essential for intracellular energy metabolism and homeostasis (Bell and Coleman, 1980). TAG and its biosynthesis have also been implicated in several important biological processes, including: in prokaryotes, yeasts and plants, as regulators of fatty acid (FA) composition of membrane lipids, as a FA source for biosynthesis of phospholipids (PLs), and as agents for remobilization of membrane lipids during senescence (Murphy, 1993; Dahlqvist et al., 2000; Alvarez and Steinbüchel, 2002); in mammals, for milk production and thermogenesis (Murphy and Vance,

1999); and, in humans, as a common element to cause some of the most prevalent diseases of the western world, hypertriglyceridemia, diabetes and obesity (Naderali et al., 2001). Recently, the identification of lipid bodies in *Toxoplasma* (Charron and Sibley, 2002) and of TAG-associated intracellular lipophilic inclusions in the sputum samples of patients infected with *Mycobacterium tuberculosis* (Garton et al., 2002) have been reported, suggesting that TAG and its biosynthesis might also have possible roles in establishing parasite infection in a host and a possible role in pathogenesis of infectious diseases. The correlation between specific bacterial or parasitic infections and lipid body formation also suggests that they might be markers of pathological changes.

The *sn*-glycerol-3-phosphate pathway (also called the Kennedy pathway) has been suggested to be the major route for de novo TAG biosynthesis in all TAG-accumulating organisms (Lehner and Kuksis, 1996). This pathway involves the stepwise acylation of *sn*-glycerol-3-phosphate and/or dihydroxyacetone phosphate to phosphatidic acid. Phosphatidic acid is then hydrolysed to *sn*-1,2-diacylglycerol (DAG). These steps are shared with the glycerophospholipid (GPL) biosynthesis. The enzyme that catalyses the final and rate-limiting step, involving the transfer of the acyl group from acyl-CoA to the *sn*-3 position of *sn*-1, 2-DAG to form TAG, is acyl-CoA:DAG acyltransferase (DGAT) (Bell and Coleman, 1980; Lehner and Kuksis, 1996). To date, two DGAT families, designated as DGAT1 and DGAT2 (which exhibit no sequence homologies to each other), have been identified in animals, fungi and plants (Cases et al., 1998; Oelkers et al., 1998; Cases et al., 2001; Lardizabal et al., 2001). In addition, a new type of DGAT, the bifunctional wax ester synthase/DGAT, has been identified in some Gram-negative bacteria, several *Mycobacterium* and *Arabidopsis thaliana* (Kalscheuer and Steinbüchel, 2003). Recently, the contribution of DGAT to mammalian TAG metabolism and its involvement in diet-induced obesity have been demonstrated using DGAT1-deficient mice (Smith et al., 2000).

The importance of TAG metabolism and its involvement in lipid homeostasis in eukaryotes and some human diseases has been well recognized. However, the implications for infectious diseases are just being discerned. In *Plasmodium* parasites, which are etiological agents for malaria, the biological significance of TAG and its metabolism is, moreover, an intriguing issue because plasmodial parasites are believed to possess little or no capacity for the oxidative degradation of FAs (e.g. β-oxidation) (Holz, 1977), although increased TAG levels have been reported in the mature forms of parasites grown in vivo and in vitro (Beach et al., 1977; Vial et al., 1982a; Vial et al., 1982b). Thus, we infer that *Plasmodium* cells use TAG for other means than as an energy source during intraerythrocytic growth. To test this theory, we performed detail characterization of TAG metabolism and trafficking through metabolic labeling, immunofluorescence and electron microscopy (EM), and enzyme activity assay.

Materials and Methods

Materials

Palmitic acid, 1, 2-*sn*-dioleoylglycerol, cholesterol (Cho), cholesteryl palmitate, brefeldin A (BFA), 6′-diamidino-2-phenylindole (DAPI), intact bovine serum albumin (IBSA) and FA-free BSA were purchased from Sigma-Aldrich (Japan); FA-free BSA was used as lipid-free BSA (LFBSA). Oleic acid, phosphatidylcholine (PC) and phosphatidylethanolamine (PE) were from Avanti Polar Lipids (AL, USA). 1,2-DAG, 1,3-DAG and TAG were from Doosan Serdary Research Laboratories (Kyungki-do, Korea). [1-^{14}C]-Oleic acid (50 mCi mmol^{-1}) and [palmitoyl-1-^{14}C]-palmitoyl-CoA (55 mCi mmol^{-1}) were from NEN Life Science Products (MA, USA) and Amersham Biosciences (Japan), respectively. Silica gel 60 thin layer chromatography (TLC) and high-performance TLC (HPTLC) plates were obtained from Merck (Darmstadt, Germany). Nile Red and Bodipy 493/503 were from Molecular Probes (OR, USA). Sudan III and trifluoperazine (TFP) from Wako Pure Chemicals (Japan). Stock solutions of IBSA, LFBSA and each lipid species used for parasite culture and metabolic labeling experiments were as described (Mitamura et al., 2000). Rabbit anti-serine repeat antigen (SERA) antiserum was prepared using the purified recombinant SE47′Δ193-225 protein (Pang et al., 1999) and purified using a protein-A column.

Parasite culture

The *P. falciparum* parasite lines used are Honduras-1 (Mitamura et al., 2000), 3D7 and Dd2 (Hanada et al., 2002). Parasite cells were routinely maintained as described (Hanada et al., 2000; Mitamura et al., 2000). Tightly synchronized cultures within a 4-hour life span were prepared for all analyses (initial parasitemia, ~0.5%; hematocrit, 3%) (Mitamura et al., 2000). The media used were: basal medium (Mitamura et al., 2000), standard medium (basal medium supplemented with 10% human serum) and serum-free medium (basal medium with 30 μM each of palmitic and oleic acids reconstituted in 60 μM LFBSA).

Parasite cultures were verified free from mycoplasma contamination using 1 ml culture for a nested polymerase chain reaction (PCR) with the primer sets provided in the Mycoplasma Detection Kit Version 2.0 (ATCC bioproduct; 90-1001K).

Metabolic labeling experiments

To measure the incorporation of radiolabeled FA into various lipid species, 5 ml tightly synchronized cultures of Honduras-1 were labeled in serum-free medium containing [^{14}C]-oleic acid (specific activity 8.3 mCi mmol^{-1}), with medium change every 12 hours. At various times, cultures were harvested thoroughly with 9 ml chilled basal medium. The precipitated erythrocytes were back-extracted for 5 minutes on ice with 9 ml solution A (basal medium supplemented with 60 μM LFBSA), followed by washing with 9 ml each of chilled solution A and basal medium. Pelleted cells were disrupted by mixing with 0.65 ml chilled deionized water using a vortex mixer. Finally, total lipids were extracted according to Bligh and Dyer (Bligh and Dyer, 1959), aliquoted and kept at 4°C until use.

For pulse-chase experiments, tightly synchronized cultures of Honduras-1 were incubated in serum-free medium, freshly changed every 12 hours. After 30 hours incubation, cultures were harvested thoroughly with an equal volume of solution A and the precipitated erythrocytes were washed once with solution A. The cells were then labeled for 4 hours in the labeling medium described above (specific activity of [^{14}C]-oleic acid, 16.6 mCi mmol^{-1}). After labeling, 5 ml cultures were harvested completely by washing with 9 ml chilled basal medium and the erythrocytes precipitated were back-extracted for 5 minutes on ice with 10 ml solution A, followed by washing twice in the same solution (10 ml). The labeled cells were chased for 20 hours in a basal medium supplemented with 60 μM IBSA without medium change. Every 4 hours after chasing, erythrocytes and culture supernatant were collected separately. All cells harvested from 5 ml culture were washed once with 9 ml chilled basal medium and then subjected to lipid extraction as described above, while the collected culture supernatant was directly used for lipid extraction.

Extracted lipid species were separated on silica gel 60 TLC plates using solvent systems of hexane/diethylether/acetic acid (70:30:1,

v/v/v) and of chloroform/methanol/acetic acid (65:25:10, v/v/v) for neutral and polar lipids, respectively. Radioactive lipid species were detected with BAS1500 image analyser (Fuji Photo Film, Japan) and their identities determined by co-migration with standard lipids. Each assigned lipid species was scraped from the TLC plate, extracted and its radioactivity measured using a liquid scintillation counter (Beckman LS6500). The incorporation value of each lipid species associated with infected erythrocyte sample was corrected against the corresponding value in uninfected erythrocyte that had been treated identically, which was used to monitor the erythrocyte capacity to incorporate the serum-derived FA into various lipid species. In the pulse-chase experiment, total radioactivity recovered in the neutral lipid fraction from cell and medium at each sampling time were comparable based on densitometry analysis [average value of the arbitrary unit was 15.488 (s.d. 1.774)]. In both experiments, the proportions of parasitized erythrocytes and parasite development were monitored microscopically using Giemsa-stained thin smears.

Measurement of neutral lipid content

Tightly synchronized cultures of Honduras-1 grown in standard medium were enriched to 92-98% mature forms by Percoll gradient. Pelleted cells were back-extracted twice in 10 ml solution A and washed twice in 10 ml basal medium before lipid extraction as described above. Extracted lipids were dissolved in 1 ml chloroform, 100 μl aliquot was used for quantification of phosphate and the rest was dried before resuspension in 20 μl chloroform for TLC analysis to quantify the neutral lipid species. Uninfected erythrocytes, treated similarly, were used for controls.

For phosphate quantification, the chloroform solution was dried, resuspended in 5 ml distilled water and 1 ml of potassium peroxodisulfate solution (0.04 g ml^{-1}), and autoclaved at 120°C for 30 minutes. To the supernatant (2.5 ml), 200 μl of developing solution {5:1 solution, v/v, of 1.44 mM *bis*-[(+)-tartrato]diantimonate[III] dipotassium trihydrate in 19.42 mM hexammonium heptamolybdate tetrahydrate: 0.409 M ascorbic acid} was added and allowed to stand for 15 minutes at 30°C. After reading the absorbance at 880 nm, the phosphate amount for every sample was determined using the potassium dihydrogenphosphate standard curve (phosphate amount, 0-5 μg; linear regression coefficient, ≥0.9991). The PL content was calculated based on one phosphate molecule for each PL species.

For quantification of neutral lipids, one-half or one-tenth of the chloroform solution prepared for TLC analysis was developed in silica gel 60 HPTLC plates using diethylether/petroleum ether/acetic acid (30:170:2, v/v/v). The plates were sprayed with 50% sulfate solution in methanol (v/v), baked for 15 minutes at 180°C and scanned with Multi Reader 1200U (NEC, Japan). The position of each lipid species were assigned using the corresponding standards and the intensity of each spot were measured with Image Master 1D Elite version 300 (Amersham Biosciences). Lipid species was quantified using the standard curves for each neutral lipid species drawn with sequential serial dilutions of a standard mixture. The linear regression coefficient of Cho (1-20 μg), cholesteryl ester (CE; 0.8-8 μg), TAG (0.8-8 μg), DAG (0.8-8 μg) and free FA (FFA; 0.8-8 μg) were ≥0.97. The molecular masses of cholesteryl oleate (651), triolein (885), diolein (621) and oleic acid (283) were used to express lipid content as micromoles.

Immunofluorescence microscopy

Aliquots of tightly synchronized cultures of Dd2, 3D7 and Honduras-1 grown in standard medium were taken at different intervals within 52 hours to monitor the changes in the staining pattern of Nile Red and Bodipy 483/503 relative to intraerythrocytic development. Nile Red and Bodipy 493/503 staining were carried out essentially as described (Greenspan et al., 1985; Gocze and Freeman, 1994). Cells were washed twice with PBS, incubated in the dark for 5-10 minutes in Hank's balanced salt solution (Invitrogen/GIBCO, Japan) with 1 μg ml^{-1} Nile Red in acetone or for 20 minutes with 10 μg ml^{-1} Bodipy 493/503 in ethanol; washed twice with Hank's balanced salt solution and stained with DAPI at 1 μg ml^{-1} for 30 minutes. Cells were imaged using either a Zeiss fluorescence microscope (Axioskop) equipped with Axiocam CCD camera or an Axioplan-2 equipped with Zeiss Pascal LSM5 laser scanning module (Carl Zeiss, Japan) both with a 100× plan apochromatic oil immersion objective (NA 1.4). Fluorescent images were acquired at identical exposure settings of 13-20 seconds with pixel values of less than 255. Line averaging using the mean of four top-to-bottom scan was used for confocal imaging. Brightfield and fluorescent images were processed using the Zeiss AxioVision or the LSM5 Pascal software with 8-bit grayscale images, the background of which were adjusted before import into Adobe Photoshop for final arrangement.

For Sudan III staining, parasites fixed in 3.7% paraformaldehyde was dropped onto uncoated, precleaned glass slides, air dried, washed three times in PBS and flooded with a working solution of Sudan III (Fukumoto and Fujimoto, 2002) for 30 minutes. Hereafter, slides were extensively washed in PBS and counterstained with DAPI before mounting using Permafluor (Immunon™). For double staining of lipid body and SERA, fixed cells were dropped onto polylysine-coated coverslips, air dried and washed three times in PBS. After 15 minutes of quenching in 50 mM ammonium chloride in PBS, cells were permeabilized in 0.05% saponin for 30 minutes and blocked with 5% BSA in solution B (PBS containing 0.1% Triton-X 100). Smears were probed with a rabbit anti-SERA antibody (Ab) and an FITC-conjugated goat anti-rabbit IgG Ab. Following 15 minutes washing with solution B, glass slides were processed for Sudan III staining as above.

Electron microscopy

Tightly synchronized cultures of Dd2 were fixed on ice for 2 hours in 2.5% (v/v) glutaraldehyde buffered at pH 7.3 in 0.1 M sodium cacodylate. Cells were washed three times in cacodylate buffer, post-fixed for 1 hour in 1% (w/v) osmium tetroxide in cacodylate buffer and rinsed in distilled water. The cells were dehydrated in an ethanol series and propylene oxide before embedding in the epoxy resin Glycidether 100 (Boehringer Ingelheim Bioproducts, Germany). Sections were sequentially stained with 2% uranyl acetate in 50% methanol and Reynolds' lead citrate before viewing in a JEM-1230 transmission electron microscope (JEOL, Japan). At least 100 sections were observed in various stages analysed.

Effect of brefeldin A and trifluoperazine treatment

For BFA treatment, BFA (5 μg ml^{-1}) or ethanol (0.1%) was added to cultures of 4-hour-old rings up to 26 hours or 30 hours. After BFA incubation at the indicated times, parasite cells were either smeared onto glass slides, stained with Nile Red or Bodipy 493/503, or washed and re-cultured in standard medium for another 6-8 hours to ensure the viability of cells after treatment.

For TFP treatment, TFP (100 μM or 500 μM) or ethanol (0.1%) was added to tightly synchronized cultures at 30 hours (mature trophozoite stage). 3 hours after incubation, parasite cells were processed as above.

DGAT activity assay

Cell lysate as an enzyme source was prepared from uninfected and *P. falciparum*-infected erythrocyte ghosts, as well as parasite cells isolated from parasitized erythrocyte by saponin treatment as described (Hanada et al., 2000) except that cells were disrupted by one-time freeze-thawing instead of sonication. When indicated, isolated parasite cells prepared by saponin treatment were disrupted through N_2 cavitation method with a 4639 cell disruption bomb from

Parr Instrument (IL, USA) (Takashima et al., 2001) and stored at –80°C until use. The DGAT activity assay was performed as described (Coleman and Bell, 1976) with slight modifications. The reaction mixture was formulated in a total volume of 150 μl containing the indicated amount of lysate, 0.5 mM 1,2-*sn*-dioleoylglycerol, 30 μM [^{14}C]-palmitoyl-coenzyme-A (specific activity 5 mCi mmol^{-1} or 13.75 mCi mmol^{-1}), 0.25 M sucrose, 1 mM EDTA, 1.8 μM LFBSA, 0-100 mM $MgCl_2$ and 100 mM Tris-HCl (pH 7.5). The enzyme reaction was started with the addition of the lysate and the assay mixture incubated for 10 minutes at ambient temperature before the reaction was terminated by adding 0.3 ml of heptane-isopropanol-H_2O solution (80:20:2, v/v/v). The lipid fraction was recovered from heptane phase after addition of 0.2 ml heptane and 0.1 ml water, dried using a vacuum concentrator, and dissolved into chloroform-methanol (1:2, v/v). The lipid species obtained were separated on silica gel 60 TLC plates using solvent systems of hexane/diethylether/acetic acid (75:25:1, v/v/v). The total amount of TAG produced was calculated by the radioactivity of the TAG spot and the final specific activity of [^{14}C]-palmitoyl-CoA used in each reaction. The radioactivity of each TAG spot was quantified by BAS2500 image analyzer (Fuji Photo Film, Japan), using the intensity of the authentic [^{14}C]-palmitoyl-CoA run in the same TLC plate as standard. A linearity of signal intensities from the different radioactivity of authentic controls was verified from 11 pCi to 11 nCi. Protein concentrations were determined by Bradford method using the Protein Assay Kit (Nippon BioRad Laboratories, Japan).

Results

Incorporation of radiolabeled fatty acid into TAGs

We have recently demonstrated that specific pairs of saturated and unsaturated FAs, the best combination of which is palmitic and oleic acids, are among the serum essential factors for the intraerythrocytic growth of *P. falciparum*, ensuring the complete cell cycle progression in vitro (Mitamura et al., 2000). The fate of these essential FAs in the intraerythrocytic parasite was investigated and its incorporation into TAG was assessed. The radiolabeled oleic acid was metabolized into various polar and neutral lipids (Fig. 1A). The incorporation into PC was preponderant (Fig. 1A) and exponential with the maturation of the parasite (Fig. 1B), corresponding to the metabolites demanded in membrane biogenesis accompanying parasite maturation (Vial et al., 1982a; Vial and Ancelin, 1998). Although the incorporation of [^{14}C]-oleic acid into TAG was ten times less efficient than that into PC, the level of TAG accumulation is significant and comparable to PE (Fig. 1B).

Incorporation of [^{14}C]-oleic acid into TAG is more stage dependent than those into PC and PE. The accumulation of TAG increased sharply from 26 hours to 38 hours, corresponding to mature trophozoite to schizont stages, after a slow lag period in the early developmental stages from 10 hours to

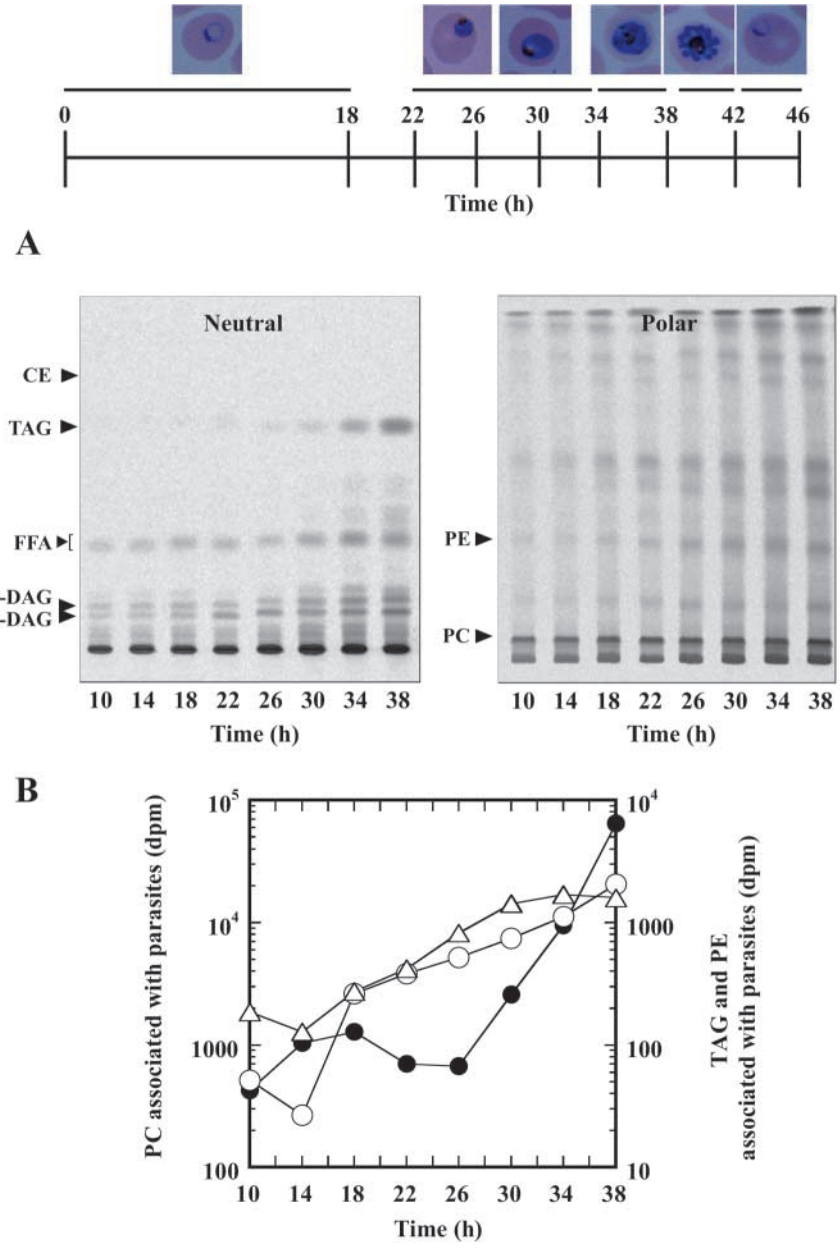

Fig. 1. Stage-specific incorporation of ^{14}C-labeled oleic acid into TAG in *P. falciparum*-infected erythrocytes. Tightly synchronized cultures of Honduras-1 were labeled and total lipids associated with infected erythrocyte were analysed. (A) TLC of the extracted total lipid species for neutral (left) and polar (right) lipids. The positions corresponding to the authentic cold lipid species are indicated: CE, cholesteryl ester; DAG, diacylglycerol; FFA, free fatty acid; PC, phosphatidylcholine; PE, phosphatidylethanolamine; TAG, triacylglycerol. (B) Kinetics of the accumulation of various lipid species incorporated with radiolabeled oleic acid in *P. falciparum*-infected erythrocytes during intraerythrocytic development. At different time points, the distribution of lipid-associated radioactivity in TAG (filled circles), PC (open circles) and PE (open triangles) are shown. Values are the total radioactivity of each lipid from 5 ml of 3% hematocrit culture. At the top is shown the dominant parasite morphology at various sampling times. One of four independent experiments displaying similar profile is shown.

26 hours (ring to young trophozoite), whereas a steady increase in PC and PE were observed (Fig. 1B). TAG accumulation also differs from that of glycosylphosphatidylinositols (GPIs), which has been shown to occur almost exclusively from early to late trophozoites, with little to none from trophozoite to schizont (Naik et al., 2000). The difference between apparent kinetics of TAG accumulation and those of PC, PE and GPIs suggests that TAG metabolism might have important implications in the later stages of the intraerythrocytic development of parasite cells.

Incorporation levels into TAG by schizont (at 38 hours) was about 150-fold higher than in ring, about three times lower and higher than PC and PE, respectively (Fig. 1B). The increase in TAG synthesis at mature stages was also observed previously using in vitro *P. falciparum* cultures and [^{3}H]-palmitate, although the exact stage of the parasite was not precisely defined (Vial et al., 1982a). Aside from TAG, 1,2-DAG and 1,3-DAG were also recovered throughout development (Fig. 1A), indicating that parasite cells have a pool of DAG, a key metabolite for both TAG and GPL biosyntheses.

The rate of degradation of ^{14}C-labeled neutral lipid associated with infected erythrocytes during the later stages in the intraerythrocytic cycle (from mature trophozoite, schizont, segmented schizont, schizont rupture, merozoite release and merozoite invasion into new uninfected erythrocyte) was determined by pulse-chase experiment. 4 hours after transfer to the chasing medium, almost 50% of cell-associated TAG was already degraded and, from 8 hours, as much as 75% (Fig. 2B). The loss of the labeled FA by the parasite is not caused by TAG excretion to the medium as we can detect only trace amount of TAG released (Fig. 2A,B). However, a significant amount of the label recovered from the medium was associated with FFA, indicating that the accumulated cellular TAG was degraded into FFA and the consequent product was released. The radioactivity associated with FFA in the medium increased linearly from 0 hours to 8 hours during the chase corresponding to the period from schizont to schizont rupture (Fig. 2B). From 12 hours to 20 hours, when merozoites start to invade new erythrocytes, enter the second cycle and develop into new rings, radioactivity associated in the FFA released to the medium reached a plateau in parallel to the observed decrease of radioactivity associated in cellular TAG (Fig. 2B). The good inverse correlation between cellular TAG degradation and release of FFA into the medium implies the existence of lipase and also probably phospholipase activities associated with the intraerythrocytic *P. falciparum*. To support this implication, the presence of various phospholipases in *Plasmodium* has been suggested (Vial and Ancelin, 1998) and a candidate gene for TAG lipase, the amino acid sequence of which showed significant homology to yeast TAG lipase (Athenstaedt et al., 1999), could be found in the *Plasmodium* database, PlasmoDB (http://plasmodb.org/).

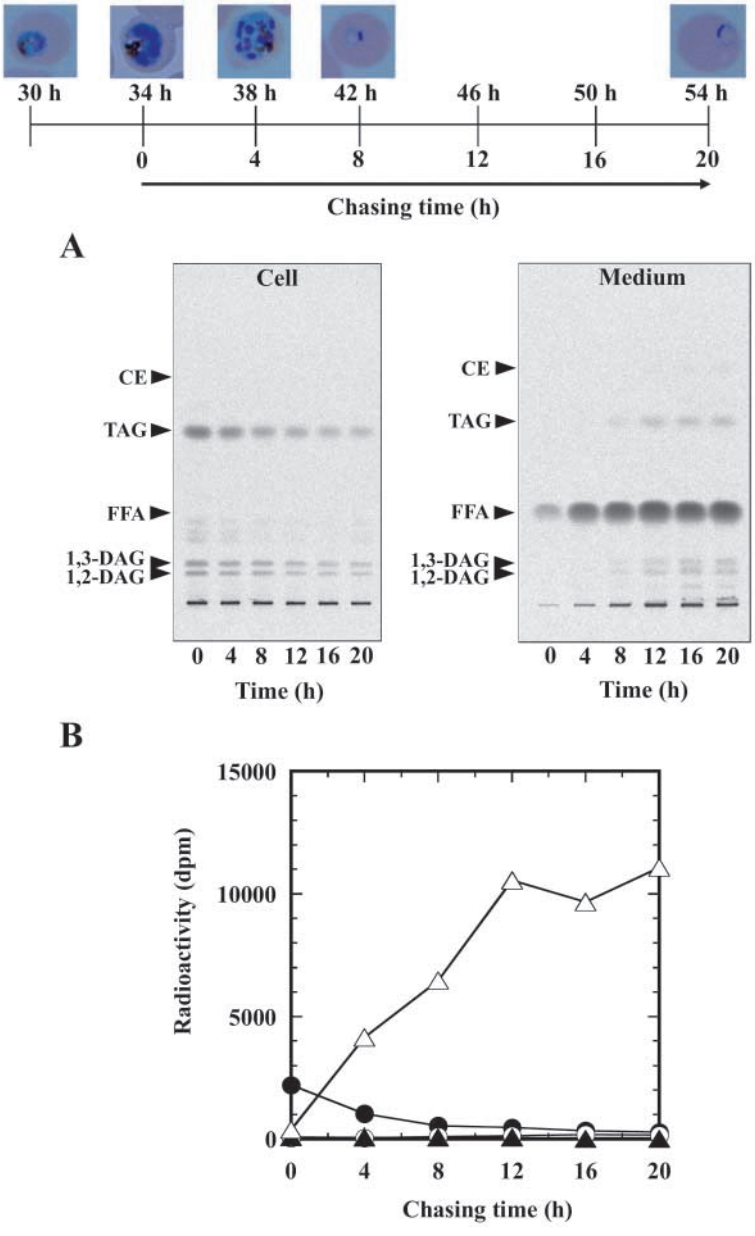

Fig. 2. Degradation of the neutral lipid pool associated with *P. falciparum*-infected erythrocytes and its release into the culture medium during the later stages of intraerythrocytic cycle. Pulse-chase experiment using tightly synchronized cultures of Honduras-1 was performed. (A) TLC of extracted neutral lipids associated with cells and released into medium. The positions corresponding to the authentic cold lipid species are indicated: CE, cholesteryl ester; DAG, diacylglycerol; FFA, free fatty acid; TAG, triacylglycerol. (B) Kinetics of TAG degradation and the release of FFA into the culture medium. At different times, the distributions of lipid-associated radioactivity in cells (filled symbols) and medium (open symbols) are shown. Values are the total radioactivity of each lipid either from the cell or from the medium of 5 ml 3% hematocrit culture. Symbols: FFA, triangle; TAG, circle. On top is shown the dominant parasite morphology at different sampling times. A representative result is shown from two independent experiments displaying similar profiles.

Composition and distribution of neutral lipid species in infected erythrocytes

To determine the extent to which the observed TAG metabolism affects the total lipid content in *P.*

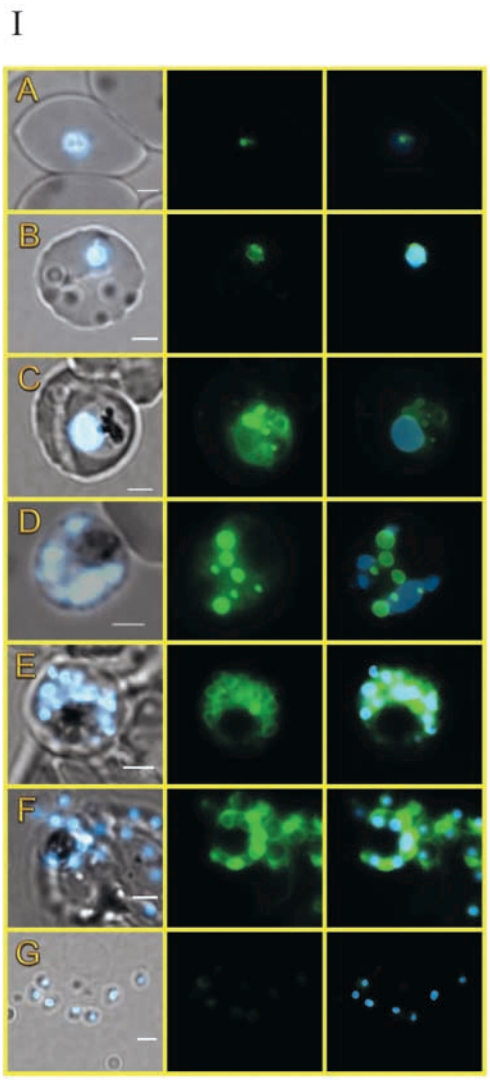

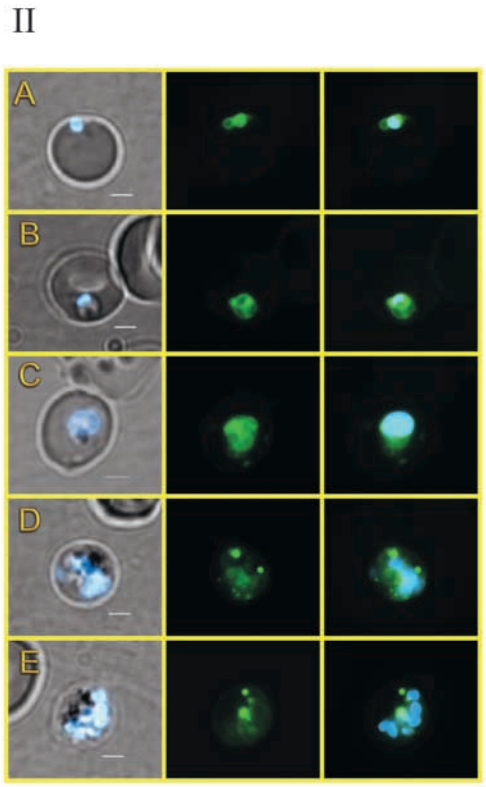

Fig. 3. Stage-dependent localization of lipid bodies in *P. falciparum*-infected erythrocyte. The erythrocytes infected with tightly synchronized Dd2 were stained with DAPI and the lipophilic dye, Nile Red (I) and Bodipy 493/503 (II) at the stages of (A) ring, (B) early trophozoite, (C) late trophozoite, (D) early schizont, (E) segmented schizont, (F) ruptured segmented schizont and (G) free merozoite. The first image in each set represents bright-field overlaid with DAPI (blue), the second is the Nile Red or Bodipy 493/503 staining (green) and the third is an overlay of lipid body fluorescence with DAPI signals. White areas denote regions of co-localization. Scale bar, 2 μm.

falciparum-infected erythrocytes, we measured the amounts of neutral and polar lipids in both mature trophozoite and schizont-rich cultures grown in standard medium. As shown in Table 1, the lipid content of mature stage parasitized erythrocyte agrees with that reported previously (Holz, 1977; Hsiao et al., 1991; Vial and Ancelin, 1998). PLs accumulated during parasite maturation accounts for 65-70% of the total lipids associated with infected erythrocyte. By contrast, with uninfected erythrocytes, the major lipids Cho and PLs account for about 50% each, with the other neutral lipids CE, TAG, DAG and FFA being barely detectable. In mature-stage parasitized erythrocytes, TAG contributed significantly to neutral lipid content. Collectively, the pattern of metabolites observed resulting from [^{14}C]-oleic acid labeling reflects the lipid distribution in infected erythrocytes grown in standard medium, although DAG and FFA could not be significantly detected under our assay conditions. The substantial increase of TAG content in segmented schizont-infected erythrocytes grown in standard medium (akin to physiological condition) compared with other neutral lipids further suggests that TAG metabolism is functional and might play some roles at the later stages of the intraerythrocytic development. Another noticeable feature with respect to the neutral lipid is the amount of Cho associated with infected erythrocytes, consistent with previous findings that Cho accumulation appears to be important to maintain intraerythrocytic proliferation (Lauer et al., 2000). The observed changes of Cho level between mature trophozoite and schizont stage parasitized erythrocytes have also been reported (Maguire and Sherman, 1990).

The levels of DAG obtained from mature-stage infected erythrocytes grown in standard medium was lower than we expected from metabolic labeling studies. Growth in serum-free medium might enhance some biosynthetic and/or degradation pathways contributing to accumulate DAG, or

Table 1. Lipid content of *P. falciparum*-infected erythrocytes

	Lipid content (μmol/10^9 cells)			
Lipid species	Uninfected erythrocytes (incubated for 30 hours)	Mature trophozoite/ early schizont (30 hours)	Uninfected erythrocytes (incubated for 34 hours)	Segmented schizont (34 hours)
Phospholipids	0.4	2.2	0.4	1.9
Neutral lipids				
Cholesterol	0.60	1.08	0.40	0.55
Cholesterol ester	<0.003	<0.008	<0.003	<0.031
Triacylglycerol	<0.002	0.045	<0.002	0.113
Diacylglycerol	<0.003	<0.008	<0.003	<0.032
Free fatty acids	<0.007	<0.018	<0.007	<0.071

Cellular lipid content of *P. falciparum*-infected erythrocytes was determined. For control, 1×10^9 uninfected erythrocytes was used. The parasitemia for 30 and 34 hour samples is 92% and 98%, respectively, with stage distribution of 45.9% mature trophozoite, 54.1% early schizonts (30 hours) and of 1.2% mid-schizonts (>4-nuclei), 98.8% segmenters (34 hours).

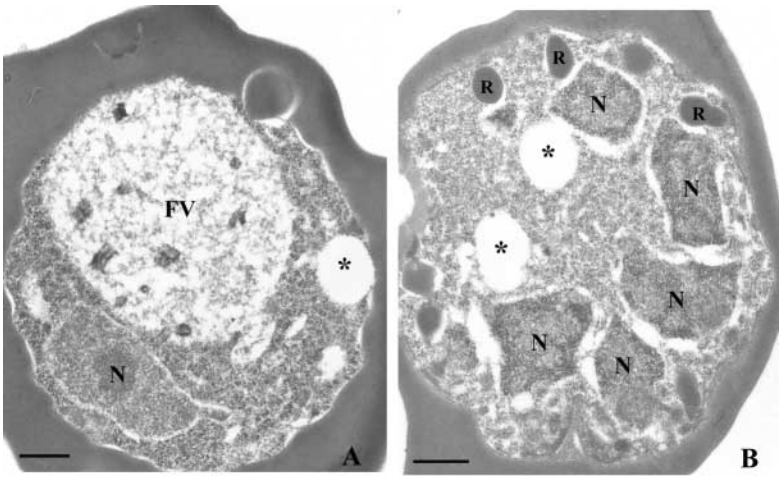

Fig. 4. Electron micrographs of lipid bodies. Mature trophozoite (A) and early schizont (B) stages of *P. falciparum*-infected erythrocytes. The presumed lipid body structure (*), nucleus (N), food vacuole (FV) and rhoptry (R) are indicated. Scale bar, 500 nm.

make certain steps in lipid metabolism become limiting, resulting into the accumulation of intermediate metabolites. The accumulation of FFA also supports this assumption.

Visualization of lipid bodies in *P. falciparum*-infected erythrocyte

In eukaryotes, stored neutral lipids accumulate as cellular lipid droplets that can be stained by the lipid body markers, Nile Red (Greenspan et al., 1985), Bodipy 493/503 (Gocze and Freeman, 1994) and Sudan III (Fukumoto and Fujimoto, 2002). As shown in Fig. 3I-II, Nile Red and Bodipy 493/503 stained small discrete bodies highly variable in size and number in *P. falciparum*-infected erythrocyte as parasite cells undergo various stages of their intraerythrocytic development. No characteristic staining pattern was observed in uninfected erythrocytes (data not shown), indicating the specific staining of lipid bodies in parasitized erythrocytes. The relative abundance and localization of lipid bodies are stage dependent. At the ring stage, fluorescence was barely detectable (Fig. 3I-II,A) but the number of cytoplasmic fluorescent droplets increased from late trophozoite with maximum abundance at schizont stage (Fig. 3I-II,C-E). When visualized together with DAPI, most fluorescent signals are close to the nucleus at the early stages of the intraerythrocytic cycle (i.e. ring to trophozoite stage) (Fig. 3I-II,A,B) but, as development proceeds, the staining patterns from both fluorescent probes became discrete. Not all lipid bodies completely overlapped with parasite nuclei as stained with DAPI and, in some instances, Nile Red and Bodipy 493/503 staining appeared to be dispersed within the parasitized erythrocyte (Fig. 3I-II,C-E), suggesting that lipid bodies are exported at the later stages. In segmented schizont, lipid bodies appears to be a 'bunch of grapes' pattern of fluorescence surrounding each nuclei, apart from some distinct, brightly homogenous fluorescence signals adjacent to them (Fig. 3I-II,E). Free merozoites observed just upon the rapture of segmented schizonts still showed the delineating pattern of fluorescence (Fig. 3I,F), whereas no merozoite released completely from the erythrocyte showed any strong fluorescence signals around cells (Fig. 3I,G), suggesting that the surrounding lipid bodies in the merozoites are degraded upon merozoite release from parasitized erythrocyte. Using 3D7 and Honduras-1, essentially the same staining pattern to that with Dd2 was observed (data not shown), indicating that the phenomena on lipid body formation and their trafficking within parasitized erythrocyte are general in *P. falciparum*.

The prominent staining of lipid bodies by Nile Red and Bodipy 493/503 opens the possibility that such structures can be observed by EM. Representative images in Fig. 4 show a distinct oval translucent structure in both mature trophozoite (A) and early shizont (B). At schizont stage, consistent with Nile Red and Bodipy 493/503 staining (Fig. 3I-II,C,D), two distinct structures were observed, although no more than four structures could be seen in sections so far examined. These distinct structures are similar not only to the one demonstrated in *Toxoplasma* (Charron and Sibley, 2002) but also to the cytoplasmic lipid droplets and/or lipid bodies purified from mammalian, yeast and fungal cells (Clausen et al., 1974; Dylewski et al., 1984; Kamisaka et al., 1999; Fujimoto et al., 2001). However, no such structures could be found in the parasitophorous vacuole (PV) from schizont and segmented schizont sections.

To substantiate, if indeed, that some lipid bodies are exported to the PV, co-localization study with a known PV-associated protein, SERA (Pang et al., 1999) was undertaken. Owing to the broad emission profile of Nile Red and Bodipy 493/503, we used Sudan III to stain lipid bodies. As shown in Fig. 5A, Sudan III gave the characteristic lipid body staining pattern as observed in Fig. 3, and the regions stained by Sudan III in schizont and segmented schizont appear to lie within the area defined by SERA, suggesting the localization of lipid bodies in the PV. Confocal microscopy, however, indicate only a partial overlap between the subcellular location of lipid bodies and SERA as examined at various slices. Although regions of partial overlap (yellow areas) are prominent in the first and central slice in schizont (Fig. 5Ba), a region of partial overlap can be observed only in the central slice in segmented schizont (Fig. 5Bb). This implies that lipid bodies show differential localization/subcompartmentation from SERA within the PV as well.

Effect of BFA and trifluoperazine on the formation and trafficking of lipid bodies

To gain mechanistic insights into the export of lipid bodies to the cytosol of *P. falciparum*-infected erythrocytes, we tested the effect of BFA, which has been shown to inhibit the transport and sorting of intracellular molecules through the parasites' endoplasmic reticulum (ER) (Elmendorf and Haldar, 1993; Benting et al., 1994; Wiser et al., 1997; Adisa et al., 2001; Hayashi et al., 2001; Wickham et al., 2001). Tightly synchronized ring stage cultures treated with 5 μg ml^{-1} BFA for 26 hours or 30 hours were compared with control cultures treated with the carrier solvent, ethanol. In control samples at 26 hours and 30 hours, when the parasites

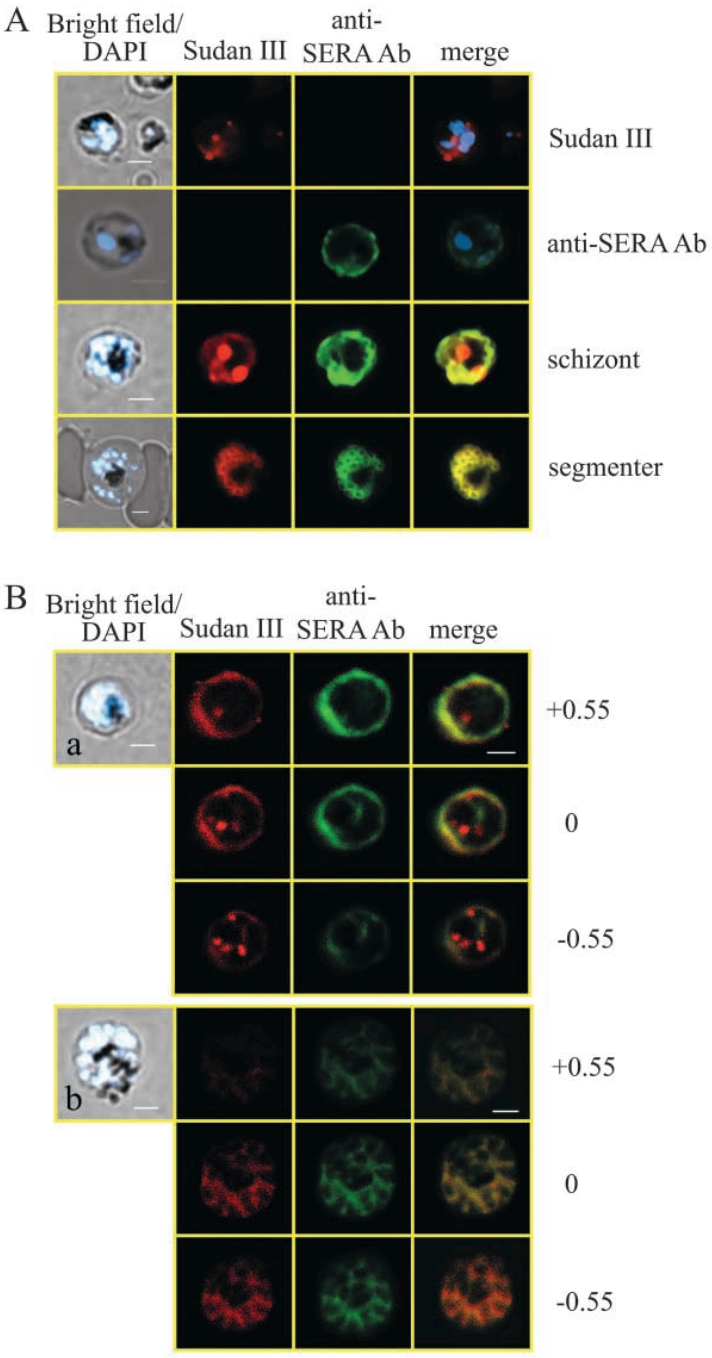

Fig. 5. Co-localization of lipid bodies with the PV marker protein SERA. (A) Fluorescent microscopic analysis of schizont-stage *P. falciparum*-infected erythrocyte stained with Sudan III and anti-SERA Ab. From left to right, panels represent bright-field overlaid with DAPI, Sudan III, SERA and overlay of Sudan III and SERA. Yellow areas denote regions of overlap. Single-stained cells (top two rows) exhibit virtually no fluorescence with the opposing filter. (B) Confocal microscopic analysis of lipid bodies and SERA co-localization in schizont (a) and segmented schizont (b). Three sections are collected through the center of the parasite by confocal microscopy. The planes on the first and third row of each set are 0.55 μm apart from the plane shown in the central row. The images, left to right, are: bright field overlaid with DAPI (blue), Sudan III (red channel), SERA protein (green channel) and merge images of red and green channels. Scale bar, 2 μm.

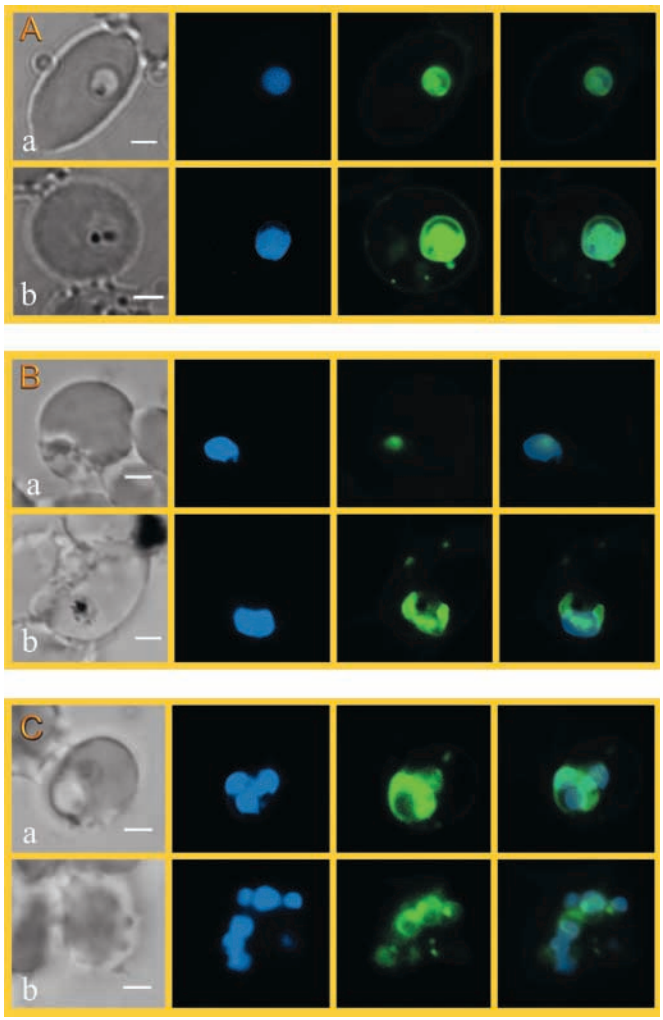

Fig. 6. Inhibition in the trafficking of Nile Red fluorescent lipid bodies with BFA. Tightly synchronized cultures of 3D7 were treated with 5 μg ml^{-1} BFA or 0.1% ethanol (solvent control) for 0-26 hours (A) or 0-30 hours (B), or re-incubated for another 8 hours after BFA treatment (C). BFA inhibition of lipid body trafficking was visualized in live parasites (a) in comparison with the corresponding control culture (b). From left to right, panels represent bright-field images, DAPI signals (blue), Nile Red staining patterns (green) and merged images of DAPI and Nile Red. White areas denote regions of co-localization. Scale bar, 2 μm.

develop into mature trophozoites, several cytoplasmic lipid droplets were localized randomly within the parasitized erythrocytes (Fig. 6Ab,Bb), as observed in Fig. 3I-II,C. Conversely, in BFA-treated samples, the number of lipid bodies was significantly reduced (Fig. 6Aa,Ba). The effect of BFA on lipid body formation and/or their trafficking in *P. falciparum*-infected erythrocytes is reversible: the treated parasites were viable and were able to continue development and lipid droplet accumulation after removal of BFA (Fig. 6C), as observed in other general secretion pathways. Although it was noted that development of the parasites was somewhat retarded by BFA treatment (approximately 4 hours delayed compared with the ethanol control, based on similar parasites as judged from DAPI and Giemsa staining), the

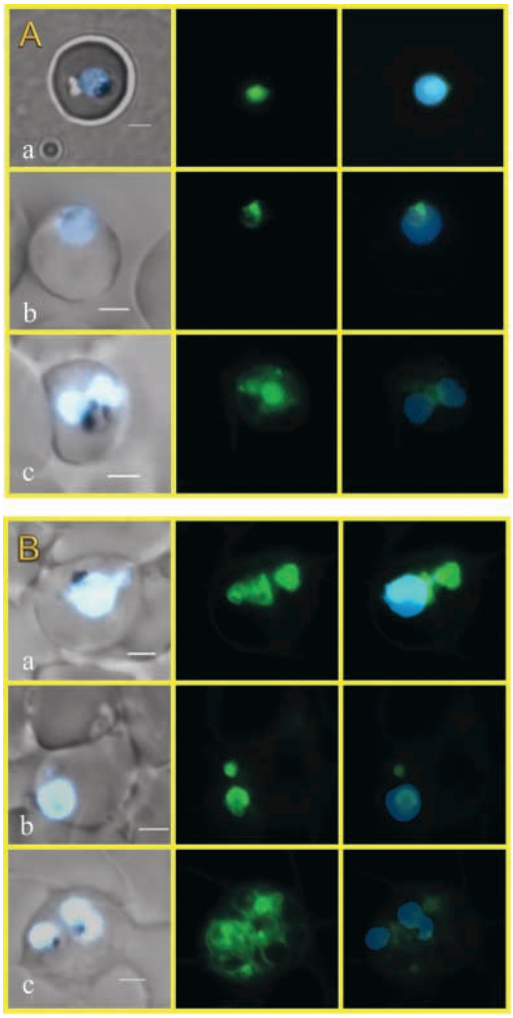

Fig. 7. Effect of TFP on the formation of Nile Red fluorescent lipid bodies. (A) Tightly synchronized cultures of Dd2 were treated with 100 μM (a) or 500 μM (b) TFP, or 0.1% ethanol (c) for 3 hours. (B) Parasite cultures treated with 100 μM (a) or 500 μM (b) TFP, or 0.1% ethanol (c) were re-cultured for another 6 hours. Panels in each set are, from left to right, bright field overlaid with DAPI (blue), Nile Red staining patterns (green) and merged images of DAPI and Nile Red. White areas denote regions of co-localization. Scale bar, 2 μm.

effect on lipid body formation and their trafficking was still significant. The effect of BFA was also observed using Bodipy 493/503 (data not shown).

Trifluoperazine (TFP), an amphiphilic cationic drug that modulates FA incorporation into TAG in fungal cells (Kamisaka et al., 1990) was added to tightly synchronized late-trophozoite stage cultures for 3 hours. Addition of TFP at 100 μM or 500 μM caused a concomitant decrease in Nile Red fluorescent lipid bodies (Fig. 7Aa,b) compared with the ethanol control (Fig. 7Ac). This effect was reversible, as evidenced by the resumption in intraerythrocytic development and lipid body accumulation when the cells were washed and recultured in standard medium (Fig. 7B). Thus, it appears that a de novo TAG biosynthetic pathway via phosphatidic acid contributes to lipid body formation in *Plasmodium*.

Table 2. DGAT activity associated with intraerythrocytic *P. falciparum*

Enzyme source	DGAT activity (pmol/min/mg)
Uninfected erythrocyte ghost	0.5±0.1
Infected erythrocyte ghost	11.4±0.3
Isolated parasite cells (ring-rich)	17.4±2.1
Isolated parasite cells (trophozoite/schizont-rich)	48.2±2.9

DGAT activity of various lysate at 20 mM Mg^{2+} was determined. Infected and uninfected erythrocyte ghost lysate (50 μg each) were prepared by freeze-thawing, whereas isolated parasite lysate (6 μg each) was prepared by N_2 cavitation. Parasitemia of the samples used for isolated parasite lysate: ring-rich (ring, 6.62%; trophozoite, 0.00%; schizont, 0.01%), and trophozoite/schizont-rich (ring, 0.51%; trophozoite, 0.38%; schizont, 1.74%). Results are average values±s.d. of triplicate.

DGAT activity associated with intraerythrocytic *P. falciparum* parasites

To obtain some information about the enzymes involved in the biosynthetic pathway for TAG in *Plasmodium*, we examined whether parasite cells retain DGAT activity using uninfected and infected erythrocyte ghost lysate as well as isolated parasite lysate as enzyme source. Infected erythrocyte ghost lysates showed significant activity compared with uninfected erythrocyte ghost lysates (Table 2), indicating that the observed DGAT activity is *P. falciparum*-infection dependent. The DGAT activity associated with infected erythrocyte ghost lysate is linear for at least 15 minutes and also directly proportional to the amounts of protein up to 50 μg (Fig. 8A,B). Unexpectedly, almost comparable activity could be detected in the reaction omitting DAG, one substrate for DGAT (Fig. 8A,B), a trend similarly observed using isolated parasite cell lysate as an enzyme source (data not shown). The high activity obtained without DAG is probably due to the assumption that freeze-thawing, which is known to disrupt membrane integrity, can release some of the free DAG associated with parasite cells, probably with the parasite membranes (Fig. 1B). Interestingly, when N_2 cavitation was used to prepare the lysate from isolated parasites instead of freeze-thawing, the DAG dependency of DGAT activity became evident, although a slight but almost constant activity could still be detected in the absence of DAG (Fig. 8C). DGAT activity was highest at around 3 mM Mg^{2+} (Fig. 8C). When compared at different parasite stages, a higher DGAT activity was detected from trophozoite/schizont-rich culture (Table 2). These results imply that the *sn*-glycerol-3-phosphate pathway at least is used in the plasmodial parasite, mainly at the trophozoite and schizont stages, consistent with the results that TAG synthesis and lipid body formation were active at trophozoite and schizont stages (Fig. 1B, Fig. 3I-II,C-E) and lipid body formation was inhibited by TFP (Fig. 7Aa,b). In addition, because N_2 cavitation is known to be among the mildest ways to maintain membrane integrity [e.g. in a study dealing with plasmodial mitochondria (Takashima et al., 2001)], these results suggest that the plasmodial DGAT enzyme and its substrate DAG are compartmentalized on parasite membranes.

Discussion

Despite detecting previously considerable amount of TAG

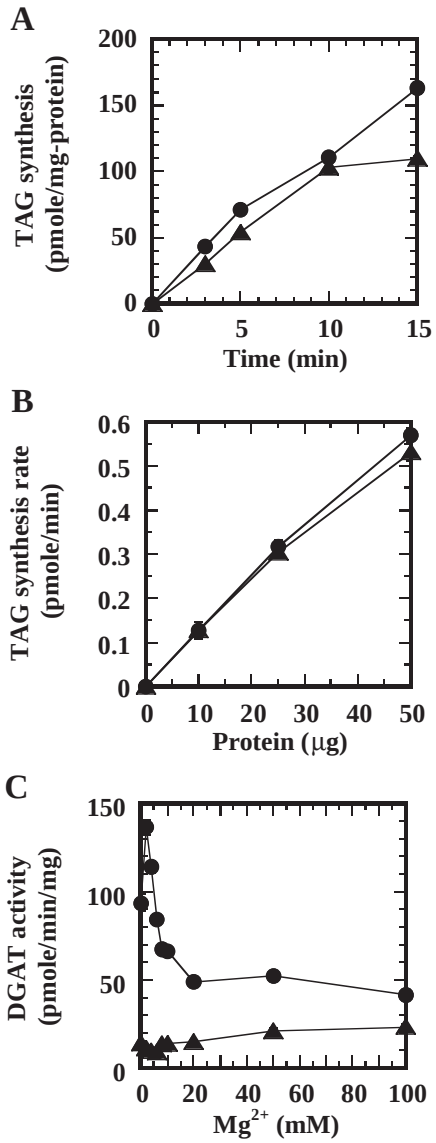

Fig. 8. DGAT activity in *P. falciparum*-infected erythrocyte ghosts and in isolated parasites. (A) Time dependence of TAG synthesis in *P. falciparum*-infected erythrocyte ghosts. TAG accumulation was monitored for 0-15 minutes from 50 μg infected erythrocyte ghost lysate at 20 mM Mg^{2+}. (B) Dependence of DGAT activity on protein concentration. TAG synthesis rate using 0-50 μg infected erythrocyte ghost lysate at 20 mM Mg^{2+} was measured. (C) Mg^{2+} dependency of the DGAT activity associated with isolated parasite cells. DGAT activity at various concentration of Mg^{2+} (0-100 mM) using 6.0 μg lysate prepared from trophozoite/schizont-rich cultures by saponin treatment and N_2 cavitation was determined. (A-C) The reaction mixtures with and without 1,2-DAG are indicated by filled circles and filled triangles, respectively; values are averages of triplicates; and s.d. for each data is indicated by error bar.

associated with intraerythrocytic parasites (Holz, 1977; Vial and Ancelin, 1998; Vial et al., 1982a; Vial et al., 1982b), there has been little interest in the study of neutral lipids, particularly TAG, probably because the observed TAG might be a product reminiscent of unnecessary metabolic pathways, considering the notion that *Plasmodium* parasites have little or no capacity for FA oxidation (Holz, 1977). The previous idea that lipid bodies serve solely as an inert lipid depot might have also contributed to this disparagement. However, the present study establishes that TAG metabolism and trafficking as a lipid body in *P. falciparum*-infected erythrocyte is indeed functioning in a stage-specific manner during the intraerythrocytic cycle given the following lines of evidence. First, intraerythrocytic parasites have the capacity to synthesize TAG actively from mature trophozoite to schizont using the serum-derived essential FAs. Second, TAG formed in parasitized erythrocytes is degraded into FFAs at the later stages, particularly from schizont to schizont rupture and merozoite release. Moreover, the FFAs formed are released into the medium during schizont rupture and/or merozoite release. Third, the intensities and numbers of lipid bodies visualized with Nile Red and Bodipy 493/503 in *P. falciparum*-infected erythrocyte increase during the course of intraerythrocytic development, reaching a maximum at the segmented schizont stage; also, at the trophozoite and schizont stages, a distinct oval translucent structure similar to those observed as lipid bodies in other living organisms could be visualized in parasite cytoplasm through EM. Furthermore, double labeling studies with the PV marker protein SERA showed that, at the schizont stage, lipid bodies appear to localize in the PV as well as the cytoplasm of parasitized erythrocyte aside from the parasite cytoplasm, suggesting that lipid bodies are secreted. Interestingly, this formation and/or secretion was reversibly impaired with BFA treatment. Fourth, *P. falciparum*-infected erythrocytes showed significant DGAT activity at the trophozoite and schizont stages, strongly suggesting that the major biosynthetic pathway for TAG in eukaryotes is active in *Plasmodium*. Taken together, we infer that the unique, dynamic cellular events regarding TAG metabolism and trafficking might participate in schizont rupture and/or merozoite release. Given that an apparently high amount of FFAs (which is likely to be attached to these membranes because of their localization within a limited area like the lipid body) has potential to cause membrane lysis, it is tempting to speculate that the concordance between the disappearance of fluorescence signal surrounding merozoite cells and release of FFAs into the medium during schizont rupture and/or merozoite release might be implicated in the disintegration of the PV membrane and/or the parasitized erythrocyte membrane. The molecular mechanism of how TAG metabolism and trafficking contributes to these particular steps, however, remains to be elucidated.

Another possible role of lipid bodies in *Plasmodium* is, as suggested in another apicomplexan parasite, *Toxoplasma* (Charron and Sibley, 2002), to serve as a place to concentrate diverted host cell lipids for the biogenesis of parasite membranes and possibly as a place for lipid metabolism to occur during intraerythrocytic proliferation of parasite cells. This, however, seems less probable because the apparently high amount of lipid body present in parasite cells disappeared during merozoite release. That TAG supplies fatty acyl chains for the synthesis of GPLs as well as GPI also seems unlikely, because much more radioactivity is incorporated into these lipids than into TAG and the observed accumulation of TAG is clearly delayed compared with that observed in these lipids (Vial et al., 1982b; Naik et al., 2002) (this study). The possibility that TAG in plasmodial cells serves as a reservoir for FAs, substrates for oxidative catabolism to generate high amount of ATP, is likewise improbable because,

when assayed in our laboratory, the capacity for β-oxidation of FA in *P. falciparum*, normalized with the activity of rat succinate dehydrogenase as a control, was at least 300-fold less (data not shown).

Microscopic observations of lipid bodies during the course of intraerythrocytic development of *P. falciparum* showed that a tiny fluorescent dot (<1 μm) at early ring stage appears to increase in size (~2 μm) and number as development proceeded to later stages. These observations suggest that a tiny lipid body in the ring serves as a nucleus to mature into a bigger lipid body. Nile Red and Bodipy 493/503 fluorescence patterns that are close to the parasite nucleus as visualized by DAPI staining might also imply a close association with the ER (Murphy and Vance, 1999). Similarly, the effect of BFA treatment on lipid body formation and/or secretion into the PV and the cytoplasm of parasitized erythrocyte suggest that lipid body formation occurs at the ER and is subsequently traffic through the Golgi to its final destination. This might imply the involvement of a classical secretion pathway for lipid body trafficking, although it is also likely that lipid bodies are associated with the cytoplasmic surface of the ER and develop as the parasite cell undergoes intraerythrocytic development. The involvement of the ER to lipid body formation and trafficking is consistent with the observations that ER membranes surround lipid bodies in *Mortierella ramanniana* (Kamisaka et al., 1999), that the ER and lipid bodies found in other eukaryotes are in close contact (Murphy and Vance, 1999) and that trafficking occurs in *Toxoplasma* lipid bodies using C4-BODIPY-C9 (Charron and Sibley, 2002). Studies using BFA to demonstrate transport and/or movement of lipid bodies in other TAG accumulating cells is, however, noticeably absent from literature.

The 'bunch of grapes' pattern of fluorescence surrounding each nucleus as it appeared in segmented schizont is intriguing, because this observation implies continuous fusion and a constant trafficking of lipid bodies to the PV, quite oppose to general observations that lipid bodies appear as distinct spherical droplets in the cytoplasm. A possible change in the physical structure and relative lipid composition of the lipid body, whether it appears as oval/round or coalescence forms, would have contributed to our inability to obtain the characteristic lipid body structure in the PV at the EM sections of schizont and segmented schizont. The unique fluorescence pattern might, however, reflect the assumed possible role of lipid bodies related to the membrane lysis described above. Spheroidal lipidic vacuoles, which appear at the periphery of the parasites at early schizonts and disappear at the onset of merozoite formation, have been observed in *Plasmodium knowlesi* schizonts by EM (Bannister and Mitchell, 1986). No further characterization, however, was made, and thus the identity of the structure observed in *P. knowlesi* and the Nile-Red-stained lipid body shown in this study remains unclear.

The results of our drug inhibition and enzyme activity assays also provide evidence for the existence of the *sn*-glycerol-3-phosphate pathway for de novo TAG biosynthesis. Although TFP can affect GPL synthesis and cause nonspecific cell damage (Kamisaka et al., 1990; Pillai et al., 2002), we speculate that, in our assay system, TFP affected lipid body formation more specifically because, upon removal of the drug and incubation in standard medium, parasite cells were able to resume normal development and lipid body formation. The high activity of DGAT, the principal enzyme in the *sn*-glycerol-3-phosphate pathway for TAG synthesis, was observed in a stage-specific manner during the intraerythrocytic development. DGAT activity associated with the intraerythrocytic parasites showed low Mg^{2+} dependency, the profile of which is similar to the mammalian DGAT2 enzyme (Cases et al., 2001); however, at higher Mg^{2+} concentrations, a significant activity could also be observed. This profile for Mg^{2+} dependency suggests the presence of a plasmodial DGAT1-like enzyme and as well as a DGAT2-like enzyme, although it is also possible that the plasmodial DGAT exhibits a peculiar Mg^{2+} dependency profile. A BLAST search in the *P. falciparum* genome revealed that there is only one candidate gene with significant homology to DGAT1, but no candidate gene for DGAT2. We therefore considered that this candidate gene might encode a plasmodial DGAT enzyme and are currently trying to express this gene in heterologous living organisms sufficient enough to characterize the enzymatic properties of the recombinant protein.

Finally, the findings demonstrated in this study could underscore unique features of *Plasmodium* parasites that might substantiate a novel biological significance of TAG, its metabolism, and trafficking in plasmodial parasites. The identification and investigation of the genes for TAG metabolism, as well as lipid body formation and trafficking would greatly facilitate studies on this interesting issue.

We thank D. Sato for helping in confocal microscopic study, K. Tai for assisting in parasite culture, E. S. Palacpac for figure preparation, Y. Kamisaka for discussion and K. Hanada for advice about metabolic labeling.

References

Adisa, A., Albano, F. R., Reeder, J., Foley, M. and Tilley, L. (2001). Evidence for a role for a *Plasmodium falciparum* homologue of Sec31p in the export of proteins to the surface of malaria parasite-infected erythrocytes. *J. Cell Sci*. **114**, 3377-3386.

Alvarez, H. M. and Steinbüchel, A. (2002). Triacylglycerols in prokaryotic microorganisms. *Appl. Microbiol. Biotechnol*. **60**, 367-376.

Athenstaedt, K., Zweytick, D., Jandrositz, A., Kohlwein, S. D. and Daum, G. (1999). Identification and characterization of major lipid particle proteins of the yeast *Saccharomyces cerevisiae*. *J. Bacteriol*. **181**, 6441-6448.

Bannister, L. H. and Mitchell, G. H. (1986). Lipidic vacuoles in *Plasmodium knowlesi* erythrocytic schizonts. *J. Protozool*. **33**, 271-275.

Beach, D. H., Sherman, I. W. and Holz, G. G., Jr (1977). Lipids of *Plasmodium lophurae*, and of erythrocytes and plasmas of normal and *P. lophurae*-infected pekin ducklings. *J. Parasitol*. **63**, 62-75.

Bell, R. M. and Coleman, R. A. (1980). Enzymes of glycerolipid synthesis in eukaryotes. *Annu. Rev. Biochem.* **49**, 459-487.

Benting, J., Mattei, D., and Lingelbach, K. (1994). Brefeldin A inhibits transport of the glycophorin-binding protein from *Plasmodium falciparum* into the host erythrocyte. *Biochem. J.* **300**, 821-826.

Bligh, E. G. and Dyer, W. J. (1959). A rapid method of total lipid extraction and purification. *Can. J. Biochem. Physiol.* **37**, 911-917.

Cases, S., Smith, S. J., Zheng, Y.-W., Myers, H. M., Lear, S. R., Sande, E., Novak, S., Collins, C., Welch, C. B., Lusis, A. J. et al. (1998). Identification of a gene encoding an acyl CoA:diacylglycerol acyltransferase, a key enzyme in triacylglycerol synthesis. *Proc. Natl. Acad. Sci. USA* **95**, 13018-13023.

Cases, S., Stone, S. J., Zhou, P., Yen, E., Tow, B., Lardizabal, K. D., Voelker, T. and Farese, R. V., Jr (2001). Cloning of DGAT2, a second mammalian diacylglycerol acyltransferase, and related family members. *J. Biol. Chem.* **276**, 38870-38876.

Charron, A. J. and Sibley, L. D. (2002). Host cells: mobilizable lipid resources for the intracellular parasite *Toxoplasma gondii*. *J. Cell Sci.* **115**, 3049-3059.

Clausen, M. K., Christiansen, K., Jensen, P. K. and Behnke, O. (1974). Isolation of lipid particles from baker's yeast. *FEBS Lett*. **43**, 176-179.

Coleman, R. and Bell, R. M. (1976). Triacylglycerol synthesis in isolated fat cell. *J. Biol. Chem.* **251**, 4537-4543.

Dahlqvist, A., Ståhl, U., Lenman, M., Banas, A., Lee, M., Sandager, L., Ronne, H. and Stymne, S. (2000). Phospholipid:diacylglycerol acyltransferase: an enzyme that catalyzes the acyl-CoA-independent formation of triacylglycerol in yeast and plants. *Proc. Natl. Acad. Sci. USA* **97**, 6487-6492.

Dylewski, D. P., Dapper, C. H., Valivullah, H. M., Deeney, J. T. and Keenan, T. W. (1984). Morphological and biochemical characterization of possible intracellular precursors of milk lipid globules. *Eur. J. Cell Biol*. **35**, 99-111.

Elmendorf, H. G. and Haldar, K. (1993). Identification and localization of ERD2 in the malaria parasite *Plasmodium falciparum*: separation from sites of sphingomyelin synthesis and implications for organization of the Golgi. *EMBO J.* **12**, 4763-4773.

Fukumoto, S. and Fujimoto, T. (2002) Deformation of lipid droplets in fixed samples. *Histochem. Cell Biol.* **118**, 423-428.

Fujimoto, T., Kogo, H., Ishiguro, K., Tauchi, K. and Nomura, R. (2001). Caveolin-2 is targeted to lipid droplets, a new 'membrane domain' in the cell. *J. Cell Biol.* **152**, 1079-1085.

Garton, N. J., Christensen, H., Minnikin, D. E., Adegbola, R. A. and Barer, M. R. (2002). Intracellular lipophilic inclusions of mycobacteria in vitro and in sputum. *Microbiology* **148**, 2951-2958.

Gocze, P. M. and Freeman, D. A. (1994). Factors underlying the variability of lipid droplet fluorescence in MA-10 Leydig tumor cells. *Cytometry* **17**, 151-158.

Greenspan, P., Mayer, E. P. and Fowler, S. D. (1985). Nile red: a selective fluorescent stain for intracellular lipid droplets. *J. Cell Biol.* **100**, 965-973.

Hanada, K., Mitamura, T., Fukasawa, M., Magistrado, P. A., Horii, T. and Nishijima, M. (2000). Neutral spingomyelinase activity dependent on Mg^{2+} and anionic phospholipids in the intraerythrocytic malaria parasite *Plasmodium falciparum*. *Biochem. J.* **346**, 671-677.

Hanada, K., Palacpac, N. M. Q., Magistrado, P. A., Kurokawa, K., Rai, G., Sakata, D., Hara, T., Horii, T., Nishijima, M. and Mitamura, T. (2002). *Plasmodium falciparum* phospholipase C hydrolyzing sphingomyelin and lysocholine phospholipids is a possible target for malaria chemotherapy. *J. Exp. Med.* **195**, 23-34.

Hayashi, M., Taniguchi, S., Ishizuka, Y., Kim, H. S., Wataya, Y., Yamamoto, A. and Moriyama, Y. (2001). A homologue of *N*-ethylmaleimide-sensitive factor in the malaria parasite *Plasmodium falciparum* is exported and localized in vesicular structures in the cytoplasm of infected erythrocytes in the brefeldin A-sensitive pathway. *J. Biol. Chem.* **276**, 15249-15255.

Holz, G. G., Jr (1977). Lipids and the malaria parasite. *Bull. WHO* **55**, 237-248.

Hsiao, L. L., Howard, R. J., Aikawa, M. and Taraschi, T. F. (1991). Modification of host cell membrane lipid composition by the intra-erythrocytic human malaria parasite *Plasmodium falciparum*. *Biochem. J.* **274**, 121-132.

Kalscheuer, R. and Steinbüchel, A. (2003). A novel bifunctional wax ester synthase/acylCoA: diacylglycerol acyltransferase mediates wax ester and triacylglycerol biosynthesis in *Acinetobacter calcoaceticus* ADP1. *J. Biol. Chem.* **278**, 8075-8082.

Kamisaka, Y., Yokochi, T., Nakahara, T. and Suzuki, O. (1990). Modulation of fatty acid incorporation and desaturation by trifluoperazine in fungi. *Lipids* **25**, 787-792.

Kamisaka, Y., Noda, N., Sakai, T. and Kawasaki, K. (1999). Lipid bodies and lipid body formation in an oleaginous fungus, *Mortierella ramanniana* var. *angulispora*. *Biochim. Biophys. Acta* **1438**, 185-198.

Lardizabal, K. D., Mai, J. T., Wagner, N. W., Wyrick, A., Voelker, T. and Hawkins, D. J. (2001). DGAT2 is a new diacylglycerol acyltransferase gene family. Purification, cloning and expression in insect cells of two polypeptides from *Mortierella ramanniana* with diacylglycerol acyltransferase activity. *J. Biol. Chem.* **276**, 38862-38869.

Lauer, S., VanWye, J., Harrison, T., Mcmanus, H., Samuel, B. U., Hiller, N. L., Mohandas, N. and Haldar, K. (2000). Vacuolar uptake of host components, and a role for cholesterol and sphingomyelin in malarial infection. *EMBO J.* **19**, 3556-3564.

Lehner, R. and Kuksis, A. (1996). Biosynthesis of triacylglycerols. *Prog. Lipid Res.* **35**, 169-201.

Maguire, P. A. and Sherman, I. W. (1990). Phospholipid composition, cholesterol content and cholesterol exchange in *Plasmodium falciparum*-infected red cells. *Mol. Biochem. Parasitol.* **38**, 105-112.

Mitamura, T. and Palacpac, N. M. Q. (2003). Lipid metabolism in *Plasmodium falciparum* infected erythrocyte: possible new targets for malaria chemotherapy. *Microbes Infect.* **5**, 545-552.

Mitamura, T., Hanada, K., Ko-Mitamura, E. P., Nishijima, M. and Horii. T. (2000). Serum factors governing intraerythrocytic development and cell cycle progression of *Plasmodium falciparum*. *Parasitol. Int.* **49**, 219-229.

Murphy, D. J. (1993). Structure, function and biogenesis of storage lipid bodies and oleosins in plants. *Prog. Lipid Res.* **32**, 247-280.

Murphy, D. J. and Vance, J. (1999). Mechanisms of lipid-body formation. *Trends Biochem. Sci.* **24**, 109-115.

Naderali, E. K., Brown, M. J., Pickavance, L. C., Wilding, J. P. H., Doyle, P. J. and Williams, G. (2001). Dietary obesity in the rat induces endothelial dysfunction without causing insulin resistance: a possible role for triacylglycerols. *Clin. Sci.* **101**, 499-506.

Naik, R. S., Davidson, E. A. and Gowda, D. C. (2000). Developmental stage-specific biosynthesis of glycosylphosphatidylinositol anchors in intraerythrocytic *Plasmodium falciparum* and its inhibition in a novel manner by mannosamine. *J. Biol. Chem.* **275**, 24506-24511.

Oelkers, P., Behari, A., Cromley, D., Billheimer, J. T. and Sturley. S. L. (1998). Characterization of two human genes encoding acyl coenzyme A: cholesterol acyltransferase-related enzymes. *J. Biol. Chem.* **273**, 26765-26771.

Pang, X.-L., Mitamura, T. and Horii, T. (1999). Antibodies reactive with the N-terminal domain of *Plasmodium falciparum* serine repeat antigen inhibit cell proliferation by agglutinating merozoites and schizonts. *Infect. Immun.* **67**, 1821-1827.

Pillai, M. G., Ahmad, A., Yokochi, T., Nakahara, T. and Kamisaka, Y. (2002). Biosynthesis of triacylglycerol molecular species in an oleaginous fungus, *Mortierella ramanniana* var. *angulispora*. *J. Biochem.* **132**, 121-126.

Smith, S. J., Cases, S., Jensen, D. R., Chen, H. C., Sande, E., Tow, B., Sanan, D. A., Raber, J., Eckel, R. H. and Farese, R. V., Jr (2000). Obesity resistance and multiple mechanisms of triglyceride synthesis in mice lacking DGAT. *Nat. Genet.* **25**, 87-90.

Takashima, E., Takamiya, S., Takeo, S., Mi-ichi, F., Amino, H. and Kita, K. (2001). Isolation of mitochondria from *Plasmodium falciparum* showing dihydroorotate dependent respiration. *Parasitol. Int.* **50**, 273-278.

Vial, H. J., and Ancelin M. L. (1998). Malarial lipids. In *Malaria: Parasite Biology, Pathogenesis, and Protection* (ed. I. W. Sherman), pp. 159-175. Washington, DC: ASM Press.

Vial, H. J., Thuet, M. J. and Philippot J. R. (1982a). Phospholipid biosynthesis in synchronous *Plasmodium falciparum* cultures. *J. Protozool.* **29**, 258-263.

Vial, H. J., Thuet, M. J., Broussal, J. L. and Philippot J. R. (1982b). Phospholipid biosynthesis by *Plasmodium knowlesi*-infected erythrocytes: the incorporation of phospholipids precursors and the identification of previously undetected metabolic pathways. *J. Parasitol.* **68**, 379-391.

Wickham, M. E., Rug, M., Ralph, S. A., Klonis, N., McFadden, G. I., Tilley, L. and Cowman, A. F. (2001). Trafficking and assembly of the cytoadherence complex in *Plasmodium falciparum*-infected human erythrocytes. *EMBO J.* **20**, 5636-5649.

Wiser, M. F., Lanners, H. N., Bafford, R. A. and Favaloro, J. M. (1997). A novel alternate secretory pathway for the export of *Plasmodium* proteins into the host erythrocyte. *Proc. Natl. Acad. Sci. USA* **94**, 9108-9113.